Volume scaling of Dirac eigenvalues in SU(3) lattice gauge theory with color sextet fermions

Thomas DeGrand[*]

Department of Physics, University of Colorado, Boulder, CO 80309, USA

Abstract

I observe a rough volume-dependent scaling of the low eigenvalues of a chiral Dirac operator in lattice studies of SU(3) lattice gauge theory with two flavors of color sextet fermions, in its weak-coupling phase. The mean value of the ith eigenvalue scales with the simulation volume $V = L^4$ as $\langle \lambda_i \rangle L^p \sim \zeta_i$, where ζ_i is a volume-independent constant. The exponent p is about 1.4. A possible explanation for this phenomenon is that p is the leading relevant exponent associated with the fermion mass dependence of correlation functions in a theory whose zero-mass limit is conformal.

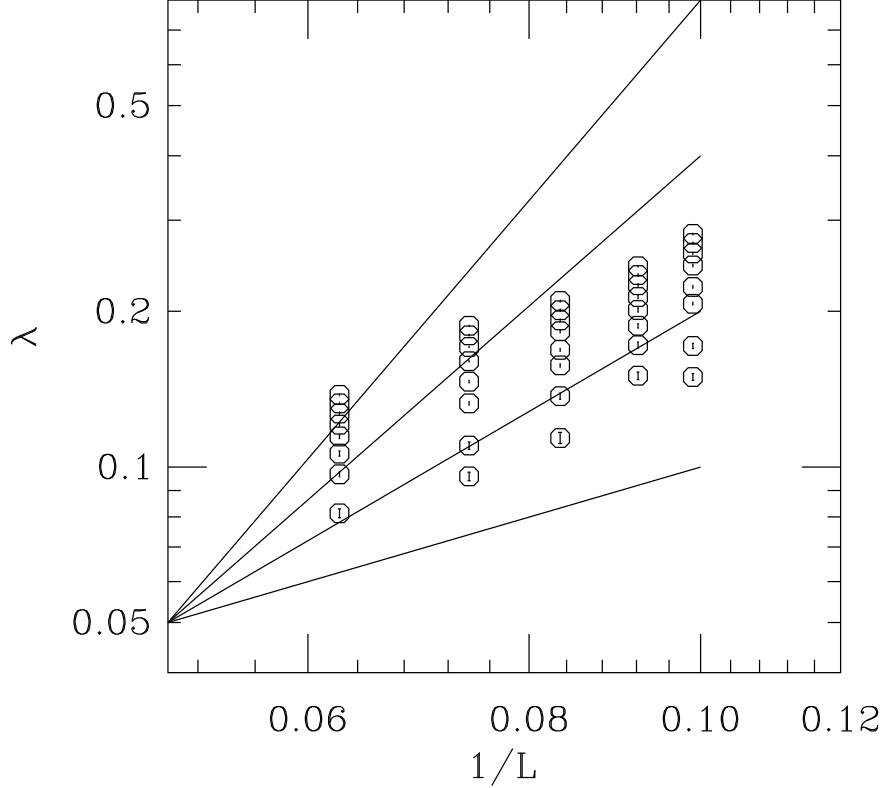[*]Electronic address: degrand@pizero.colorado.edu

FIG. 1: Average values of 8 lowest eigenvalues of the sextet-representation valence overlap operator, vs $1/L$, where the lattice volume V is defined to be $V = L^4$. The actual volumes, moving from left to right across the graph, are 16^4, $16^3 \times 8$, 12^4, $12^3 \times 8$ and $12^3 \times 6$. The four lines are scaling curves $\langle \lambda_i \rangle L^p = $ constant, for $p = 4, 3, 2, 1$, from the top of the figure down.

I.   INTRODUCTION

Recently, various research groups [1, 2, 3, 4, 5, 6, 7, 8, 9, 10, 11, 12, 13, 14, 15, 16] have begun to use lattice methods to study field theories which might be candidates for strongly coupled beyond - Standard Model phenomena [17]. These models typically involve gauge fields and a large number of fermion degrees of freedom, either many flavors of fundamental representation fermions (where the discussion goes back to Refs. [18, 19]) or a smaller number of flavors of higher-dimensional representation fermions (strongly emphasized by Refs. [20, 21, 22]).

I have been part of a collaboration studying SU(3) lattice gauge theory with two flavors of color sextet fermions[5, 11]. This theory has a weak-coupling phase which is deconfined and chirally restored. Recently, I observed a peculiar volume-dependent scaling of the eigenvalues of a valence quark Dirac operator, in the weak coupling phase. Fig. 1 shows this result. This is very different from the spectrum in simulations with fundamental representation fermions. A presentation of the dependence, a comparison with simulations of two flavors of fundamental representation fermions (which do not show this scaling dependence), and a possible explanation, are the subjects of this paper.

I begin with some (possibly) relevant background: The usual description of renormalization for a gauge theory coupled to massless fermions generally concentrates on the behavior

of the running gauge coupling, and makes a distinction about how the gauge coupling flows under rescaling to the infrared: it could flow to strong coupling in the case of a confining theory, or to zero, for a trivial theory, or to a fixed point at some nonzero value, g^{2*}. The latter case is referred to as an infrared-attractive fixed point (IRFP) theory. This is a phase with no confinement, no chiral symmetry breaking, and algebraic decay of correlation functions (no particles). Evidence has been presented that several such theories exist: $SU(3)$ gauge theory with $N_f = 12$ flavors of fundamental fermions [4, 14], $SU(3)$ gauge theory with $N_f = 2$ flavors of sextet fermions (the subject of this paper) [5] and $SU(2)$ gauge theory with $N_f = 2$ flavors of adjoint fermions[15].

While for confining theories the gauge coupling is relevant (the Gaussian fixed point $g = 0$ is unstable), that is not the case for IRFP theories. The gauge coupling (more precisely the distance of the bare gauge coupling from its fixed point value $(g^2 - g^{2*})$) is an irrelevant coupling. The critical surface encompasses a wide range of values of bare gauge couplings, plus the values of any other irrelevant operators (in a lattice theory, these are the usual lattice artifacts). The relevant coupling of an IRFP theory is the fermion mass, which must be fine-tuned at the UV scale to reach the critical surface (i.e. $m_q = 0$). How a nonzero fermion mass drives the lattice theory off the critical surface determines the asymptotic behavior of (nearly) all correlation functions. The situation is completely equivalent to that of an order-disorder transition in a magnetic system. The only difference is that the relevant direction is parameterized by the quark mass m_q, rather than the reduced temperature $t = (T - T_c)/T_c$ of the magnet. (A closer analogy is to a system which has been fine tuned to its Curie point and then placed in an external magnetic field. The external field breaks the underlying global symmetry just as a quark mass explicitly breaks chiral symmetry.) [23]

The framework to describe the physics of these systems is also standard. Tuning the mass to zero causes the correlation length to diverge algebraically,

$$\xi \sim m_q^{-\frac{1}{y_m}}. \tag{1}$$

As m is tuned to zero, the singular part of the free energy scales as

$$f_s(m_q) = m_q^{D/y_m}(A_1 + A_2 m_q^{|y_i|/y_m}). \tag{2}$$

where D is the system's dimensionality (here $D = 4$) A_1 and A_2 are non-universal constants and y_i is the biggest non-leading exponent. This is most likely the exponent y_g of the gauge coupling, $g^2 - g^{2*}$, which can be determined from the beta function as measured in (for example) Schrodinger functional simulations at $m_q = 0$.

How can one measure y_m? The most direct way is through the correlation length ξ, through Eq. 1. In a finite simulation volume, ξ will obey Eq. 1 until it grows to be the order of the size of the lattice, and then will saturate. To observe Eq. 1 probably requires large volumes.

Unitarity bounds for conformal field theories[24] constrain the critical exponent of the condensate, $\langle \bar{\psi}\psi \rangle = \Sigma$,

$$\Sigma(m_q) = \frac{\partial f_s}{\partial m_q} \sim m_q^\gamma \tag{3}$$

to lie in the range $3 > \gamma = D/y_m - 1 > 1$. (Note that for $D = 4$, γ is defined to be $3 - \gamma_m$ where γ_m is the anomalous dimension for the fermion mass.) For $D = 4$ this means that the allowed range of y_m is between 1 (free field behavior, all exponents except y_g given by dimensional analysis) and 2. This make a measurement of y_m through the mass dependence

of the condensate problematic. The condensate has a UV-sensitive piece proportional to the quark mass [25], and so $\langle \bar{\psi}\psi \rangle \sim C_1 m_q + C_2 m_q^\gamma + \dots$. This masks the m_q^γ non-analytic behavior. This is quite similar to the situation in finite temperature QCD, precisely at $T = T_c$, where[26]

$$\Sigma(a, m_q, T) \sim c_1 m_q/a^2 + c_\delta m_q^{1/\delta} + \text{analytic}. \tag{4}$$

It is different from QCD in that for the IRFP theory there are no Goldstone bosons (which contribute their own non-analytic piece to the condensate, below T_c). It is also different from QCD in that while in QCD, Eq. 4 applies only at T_c, in an IRFP theory Eq. 4 gives the behavior of the condensate throughout the basin of attraction of the IRFP. Worryingly, the expected result from $D = 3$ $O(4)$ universality, $1/\delta = 1/0.56 = 1.78$, implies that the QCD number is smaller than the smallest unitarity bound, meaning that the QCD susceptibility would then be more singular than in a conformal theory. However, the QCD susceptibility does not seem to have been measured yet [27].

The way I choose to attack y_m through the condensate involves the Banks-Casher relation[28], which relates the condensate to the density of eigenvalues λ of the Dirac operator $\rho(\lambda)$. At nonzero mass it is

$$\Sigma(m_q) = -\int \rho(\lambda)d\lambda \frac{2m_q}{\lambda^2 + m_q^2}. \tag{5}$$

If the theory is conformal, and $\Sigma(m_q) \sim m_q^\gamma$, then $\rho(\lambda)$ also scales as λ^γ. The search for the effect I saw was motivated by a finite-size scaling argument[29] which relates the scaling for the density ρ to the scaling of the value of individual eigenvalues. If we consider the average value of the ith eigenvalue of the Dirac operator in a box of volume $V = L^D$, and if $\rho(\lambda) \sim \lambda^\gamma$, then we expect

$$\langle \lambda_i \rangle \sim \left(\frac{1}{L}\right)^p \tag{6}$$

where the exponent is

$$p = \frac{D}{1 + \gamma}. \tag{7}$$

(A quick derivation: $\rho \sim \lambda^\gamma$ means that eigenvalues are uniformly distributed in an $N = \gamma + 1$ dimensional space of volume $V = R^N$,

$$\lambda = \frac{\pi}{R}(\sum_{i=1}^{N} n_i^2)^{1/2} \quad n_i = 1, 2, \dots R \tag{8}$$

so an eigenvalue scales as $\lambda_i \sim 1/R = (1/V)^{\frac{1}{N}} = (1/V)^{\frac{1}{\gamma+1}}$. Now suppose we are in D physical dimensions; in a box of volume V, there are $V = L^D$ modes, from which Eq. 7 is obtained. One example of this formula is free field theory: $\gamma = D - 1$ and $p = 1$. Another is the case of chiral symmetry breaking encoded in the usual formulas of its Random Matrix Theory analog: $\gamma = 0$ so $\rho(\lambda) \to \rho_0$ a constant, and $p = D$. This is an eigenvalue spectrum which depends on the dimensionless product $\lambda \Sigma V$ or $\langle \lambda_i \rangle \sim 1/V$.)

For the case of an IRFP theory, p is equal to y_m, the leading exponent. A way to determine y_m is through the volume dependence of eigenvalues of the Dirac operator.

There are several problems associated with carrying out this proposal. The first is numerical. Lattice discretizations of the Dirac operator which are easy to implement (allowing

simulations on large volume) break the full $SU(N_f) \otimes SU(N_f)$ chiral symmetry of the continuum Dirac operator. This complicates the analysis. For example, for the fermions in my simulations (Wilson-type fermions), explicit chiral symmetry breaking in the action introduces an additive shift to the eigenvalues. For a cleaner test of Eq. 6, I will use partial quenching: I will take configurations generated with lattice fermions which do not have exact chiral symmetry, and measure the Dirac spectrum using an implementation of lattice fermions with exact chiral symmetry (overlap fermions). This raises another issue: is what the valence fermion sees a faithful realization of what is happening in the equilibrium distribution of real dynamical variables? I think that for a first study, what I am going to do is adequate.

The next problem involves interpreting the results. For the case of a system which exhibits chiral symmetry breaking, there is a tight theoretical description of the behavior of the lowest eigenvalues of the Dirac operator, which allows one to relate delicate features of the spectrum to the low energy constants of the theory (the condensate, the pseudoscalar decay constant, and possibly others). This description is based on Random Matrix Theory (RMT). It is quite straightforward to use Random Matrix Theory predictions to tell whether a system exhibits chiral symmetry breaking. Conversely, if a system is in a chirally-restored phase, there are no longer RMT predictions to compare results against.

I already know that our target theory has a weak-coupling phase which is deconfined and chirally-restored. The restoration of chiral symmetry is observed through regularities in the spectrum of screening masses as well as the behavior of the pseudoscalar decay constant as a function of quark mass. I can only continue while using the simplest properties of the eigenvalues, namely their scaling with system size.

Now I return to a fuller description of Fig. 1. This is a plot of the average value of the ith eigenvalue of the valence overlap operator versus simulation volume, plotted using $L = V^{1/4}$. The data are all collected at the same values of the bare parameters, in the deconfined phase and at a quark mass where the lattice volume causes the correlation length to saturate. The actual volumes, moving from left to right across the graph, are 16^4, $16^3 \times 8$, 12^4, $12^3 \times 8$ and $12^3 \times 6$. Clearly, the spectrum does not appear to depend on much beside the volume, and it seems to show scaling, $\langle \lambda_i \rangle \sim L^{-p}$.

The four lines are scaling curves $\langle \lambda_i \rangle L^p = $ constant, for $p = 4, 3, 2, 1$, from the top of the figure down. $p = 4$ would be the scaling curve if chiral symmetry were broken. $p = 1$ is free-field behavior. The data appear to lie in between – in fact, the best fit value is about $p = 1.4$.

Svetitsky, Shamir and I have already observed (but with a different lattice discretization) that $SU(3)$ $N_f = 2$ sextet QCD shows evidence for an IRFP [5]. If that observation survives future tests, the exponent p is indeed y_m, the leading relevant exponent. If that observation turns out to be false, the volume scaling of eigenvalues is still something striking. It is different from what is seen in the deconfined phase $SU(3)$ $N_f = 2$ fundamental QCD (as we will see, below).

The data in Fig. 1 all come from simulations at one set of bare parameters. However, if the simulations were in fact done in the basin of attraction of the IRFP, irrelevancy of the gauge coupling means that different gauge couplings merely correspond to lattice actions with different amounts of scaling violations.

Finally, the idea behind this calculation was first described by the authors of Ref. [9]. They proposed doing simulations with dynamical chiral fermions (overlap fermions) so that the Dirac operator whose eigenvalues are measured is the same one that appeared in the

action. They performed these simulations, also in the deconfined phase of $SU(3)$ $N_f = 2$ sextet QCD. They identified that the eigenvalue spectrum was inconsistent with expectations for the behavior of a system with chiral symmetry breaking, but only studied one volume (6^4 lattices).

The paper proceeds as follows. In Sec. II I describe details of the simulations. In Sec. III I provide some background: I examine whether lattice data show evidence that the gauge coupling is irrelevant. I make a direct attack on the correlation length exponent using Eq. 1. I find numbers also in the range 1.5-1.6. I then make some comparisons of $N_f = 2$ fundamental and sextet QCDs in their deconfined phases. These systems are quite different. In Sec. IV I provide background for Fig. 1 and describe my attempts to pin down the exponent p. I conclude with some speculations and (rather obvious) suggestions for follow-up work.

II.   NUMERICAL TECHNIQUES

I performed simulations on a system with $SU(3)$ gauge fields and two flavors of dynamical fermions in the symmetric (sextet) representation of the color gauge group. The lattice action is defined by the single-plaquette gauge action and a Wilson fermion action with added clover term [30]. The fermion action employs the differentiable hypercubic smeared link of Ref. [31], from which the symmetric-representation gauge connection for the fermion operator is constructed. No tadpole-improvement is used and the clover coefficient is set to its tree-level value. The bare parameters which are inputs to the simulation are the gauge coupling $\beta = 6/g^2$, the fermion hopping parameter κ. The integration is done with one additional heavy pseudo-fermion field as suggested by Hasenbusch [32], multiple time scales [33], and a second-order Omelyan integrator [34].

The routines for simulating sextet-representation fermions were developed with (and mostly by) B. Svetitsky and Y. Shamir. The dynamical fermion algorithm was adapted from a program written by A. Hasenfratz, R. Hoffmann and S. Schaefer[35]. All computer code is based on the publicly available code of the MILC collaboration [36].

Simulation volumes range from $12^3 \times 6$ to 16^4 sites, and typical data sets range from a few hundred to a thousand trajectories. I recorded lattices every five trajectories (of unit simulation time trajectory length) and collected 40-80 lattices per parameter set for the calculation of screening lengths and overlap eigenvalues.

The trick of combining periodic and anti-periodic boundary conditions for valence quarks [37, 38, 39, 40] is used in spectroscopy or screening mass measurements.

Throughout this work, instead of quoting κ, I will use the the Axial Ward Identity (AWI) quark mass, defined through

$$\partial_t \sum_x \langle A_0(x, t) X(0) \rangle = 2m_q \sum_x \langle P(x, t) X(0) \rangle . \tag{9}$$

where $A_0 = \bar{\psi}\gamma_0\gamma_5\psi$, $P = \bar{\psi}\gamma_5\psi$, and X is any source. (I temporarily drop factors of the lattice spacing in the derivations.) The derivative is taken to be the naive difference operator $(\partial_\mu f(x) = (f(x + \hat{\mu}a) - f(x - \hat{\mu}a))/(2a))$.

The valence Dirac operator whose eigenvalues are the subject of this study is the overlap operator [41, 42]. Details of the particular implementation of the action are described in Refs. [43, 44, 45, 46, 47]. The only new ingredient is the application to symmetric-representation fermions, using the same combination of hypercubic link and projection as

for the dynamical fermions. Eigenvalues of the squared Hermitian Dirac operator $D^\dagger D$ are computed using the "Primme" package of McCombs and Stathopoulos[48] and split apart in the usual way.

There are potential problems with this analysis. The first one involves the index theorem, relating the winding number of the gauge field k to the number of Dirac fermion zero modes,

$$\text{index} = 2T(R)k. \tag{10}$$

$T(R)$ is the Dynkin index of the representation R, $1/2$ for fundamental representation fermions, $(N + 2)/2$ for sextet fermions in the color group $SU(N)$, and so on. Thus we expect to see multiples of 5 zero modes for adjoint overlap fermions in our $SU(3)$ case.

However, ten years ago Heller, Edwards, and Narayanan discovered[49] that the index theorem applied to adjoint overlap fermions in background $SU(2)$ gauge configurations failed: here $2T(R) = 4$ and they saw configurations with zero modes which were not multiples of four. Similar results were more recently reported by Garcia Perez, Gonzalez-Arroyo and Sastre[50]. Nógrádi reported similar behavior from simulations with $SU(3)$ sextet fermions[51] and in simulations where the bare gauge coupling is large, I have seen configurations whose zero mode content was a not a multiple of 5.

It is unknown whether this is a disease, just a particular failure of the overlap action to capture topology when the gauge configuration is rough, or real physics, something which persists in a continuum limit. I am going to ignore it. The gauge configurations at the parameter value used to construct Fig. 1 were smooth enough that all of the lattices I collected for Fig. 1 had $Q = 0$.

The second potential problem concerns possible phase structure in the theory. In Ref. [11] we observed that in the deconfined phase of sextet QCD, the Polyakov loop ordered in one of the negative real directions, roughly along one of the complex elements of $Z(3)$ ($\text{Re}\,\langle\text{Tr}\,P(x)\rangle < 0$, $\text{Im}\,\langle\text{Tr}\,P(x)\rangle \neq 0$). This is quite different behavior from fundamental QCD, where the Polyakov loop orders positively ($\text{Re}\,\langle\text{Tr}\,P(x)\rangle > 0$, $\text{Im}\,\langle\text{Tr}\,P(x)\rangle = 0$). It is likely that there is a complicated phase structure as a function of the bare parameters, with different vacua favored in different regions of the bare parameter space [52]. Detailed studies of the phase structure (at smaller volumes) are currently being performed by Machtey, Shamir, and Svetitsky [53]. For the time being, I believe, based on my simulations, that the equilibrium small quark mass region is $\text{Re}\,\langle\text{Tr}\,P(x)\rangle < 0$. I checked that all the data in Fig. 1 remained in the $\text{Re}\,\langle\text{Tr}\,P(x)\rangle < 0$, $\text{Im}\,\langle\text{Tr}\,P(x)\rangle \neq 0$, phase during their time histories.

III. SOME SPECTROSCOPIC CHECKS

Before analyzing eigenvalues, I pause to consider some potential complications.

A. Does the gauge coupling appear to be irrelevant?

If the gauge coupling is irrelevant, observables collected at different values of the bare coupling will show small differences, qualitatively similar to the different sizes of scaling violations seen in ordinary QCD simulations when different lattice actions are used.

We [11] saw this behavior in our earlier work, but did not describe it as such. It is easy to overlay screening masses taken in the deconfined phase at different values of β (at identical lattice volumes) and observe that they coincide. I now show a variation of that comparison.
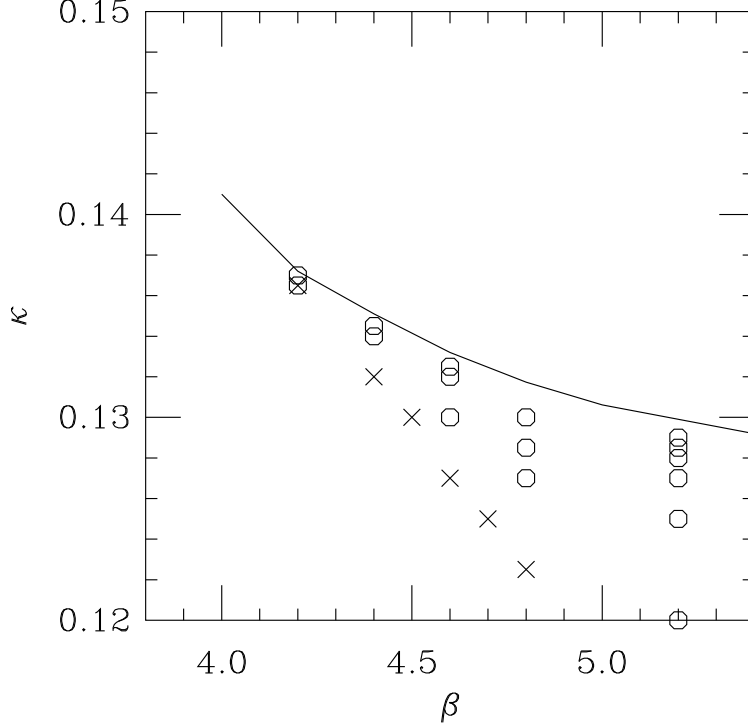
FIG. 2: Map of the bare coupling constant plane relevant to our sextet simulations. The solid line is the line of zero quark mass, $\kappa = \kappa_c$. The crosses show the location of the confinement-deconfinement crossover at $N_t = 6$. Octagons show the data collection points for the next figures.

To begin, the phase diagram of the present system is shown in Fig. 2. The line is the location where the AWI quark mass vanishes, $\kappa = \kappa_c$. The crosses show the location of the $N_t = 6$ deconfinement transition. To the left of the crosses, the theory confines and (to the extent we can discuss this for massive quarks) chiral symmetry is broken; to the right, the theory is deconfined and chiral symmetry is restored. Octagons show the data collection points (all on $12^3 \times 6$ volumes) for the next figures. I have checked that all data collected at larger volumes (all at $\beta = 5.2$) is deconfined, but have not accurately mapped the phase boundary.

I define the correlation length ξ to be the inverse of the screening mass in the pseudoscalar channel and plot ξ vs $1/m_q$, the inverse AWI fermion mass, in Fig. 3. (In the deconfined phase, the pseudoscalar, vector, axial vector and scalar screening masses are essentially degenerate.) The data show that the correlation length is dominantly driven by $1/m_q$, much less by the gauge coupling β.
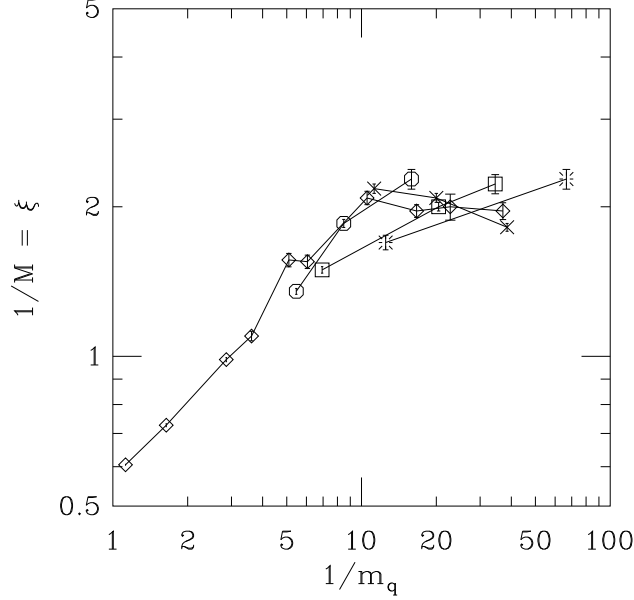
FIG. 3: Correlation length (inverse pseudoscalar screening mass) vs inverse quark mass for $N_f = 2$ sextet fermions on a $12^3 \times 6$ volume. Bursts are $\beta = 4.2$; crosses, $\beta = 4.4$; squares, $\beta = 4.6$, octagons, $\beta = 4.8$, and diamonds, $\beta = 5.2$. Lines connect points with the same β values.

B. Contrasting the deconfined phase for $N_f = 2$ fundamental fermions

The reader might recall a fact about screening masses in the deconfined phase of fundamental representation QCD: they scale with system size like [54]

$$m_H^2 = 4 \left[\left(\frac{\pi}{N_t} \right)^2 + m_q^2 \right] \tag{11}$$

where $\frac{\pi}{N_t}$ is the lowest nonzero Matsubara frequency associated with antiperiodic boundary conditions in a lattice of temporal length N_t. The data in Fig. 3 are for $N_t = 6$, for which Eq. 11 predicts $m_H = 2\pi/6 \sim 1$ in the chiral limit. The limiting value of m_H is about half that value. In fact, Eq. 11 does not reproduce any of the data. The situation at the one β value (5.2) where I have many volumes, ranging from $12^3 \times 6$ to 16^4, is shown in Fig. 4. The limiting correlation length does not seem to depend separately on N_t; rather, it appears to increase as the lattice volume increases.

C. Scaling of correlation lengths?

In the infinite volume limit we expect that the mass gap will disappear at vanishing fermion mass. The chiral susceptibility $\chi = \partial \Sigma(m_q)/\partial m_q$ is related to the volume integral of the isosinglet correlator $C(x) = \langle \bar{\psi}\psi(x)\bar{\psi}\psi(0) \rangle$. When the lightest mass in this channel vanishes, the susceptibility will diverge. As in QCD, this argues that the screening mass in this channel should vanish. Again, as in QCD, the calculation of isosinglet correlators is difficult due to the presence of disconnected diagrams, so as a first try I will mimic the
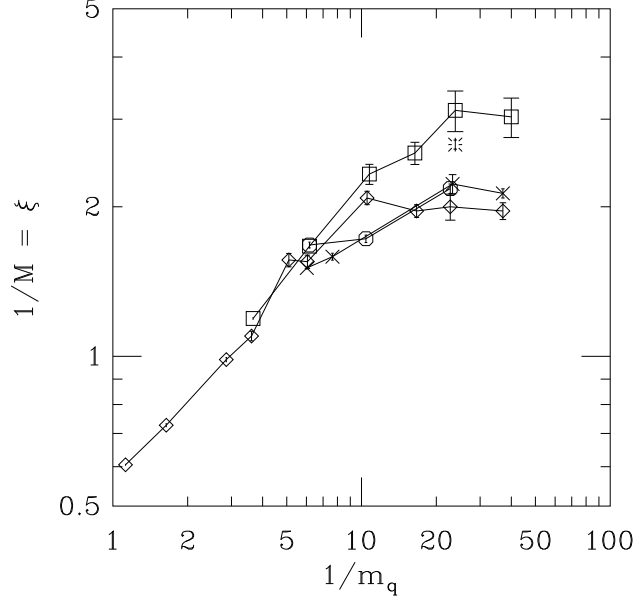
9

FIG. 4: Correlation length (inverse pseudoscalar screening mass) vs inverse quark mass for $N_f = 2$ sextet fermions at $\beta = 5.2$. Diamonds, $12^3 \times 6$ volume; octagons, $12^3 \times 8$ volume. crosses, 12^4 volume; squares, $16^3 \times 8$ volume, and burst, 16^4 volume. Lines connect points with the same β values.

QCD analysis [55] and look at the isotriplet scalar correlator. Just because the data is quite accurate, I will also look in the pseudoscalar channel.

Fig. 4 shows us that data from different volumes seem to lie on a volume independent curve until the correlation length reaches a size comparable to the system size. Presumably the relation between rounding of the correlation length and volume is geometry dependent. So I will work with the two data sets I have, which have the same aspect ratio, $12^3 \times 6$ and $16^3 \times 8$. I will try a fit of the form of Eq. 1, varying the range and composition.

A pair of representative fits are shown in Fig. 5. The left panel is the pseudoscalar and the right panel the scalar; I will define an exponent through $1/m_j \sim (1/m_q)^{1/y_j}$ with $j = \pi$ or a_0. For the pictured fits the results are $y_\pi = 1.66(6)$, $\chi^2 = 41.7/7$ dof (pseudoscalar) and $y_{a_0} = 1.54(5)$, $\chi^2 = 9.7/7$ dof (scalar). It is relatively easy to find ranges of fits for the scalar mesons for which $\chi^2 < 10$ with $1/y_{a_0}$ drifting from .51(2) to .67(3) according to the fit range. The pseudoscalar data has smaller uncertainty and hence poorer confidence levels, $\chi^2/$dof between 3-4 for 4-9 points, and $1/y$ ranging from 0.57(1) to 0.62(2). My data do not have the dynamic range to take my result too seriously. (If people had not spent the last 30 years fitting $m_\pi^2 \sim m_q$ in QCD over the same range of masses, I would not have tried it.) Researchers with larger simulation volumes might like to attempt this, however.
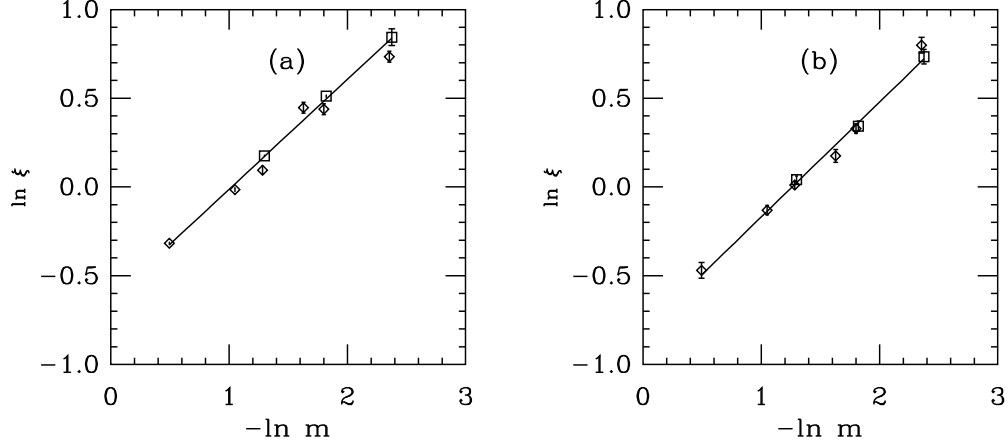
FIG. 5: Representative fits to (a) pseudoscalar and (b) scalar correlation lengths. Data are diamonds for $12^3 \times 6$ volumes and squares for $16^3 \times 8$ volumes.

IV. DISCUSSION OF RESULTS FROM EIGENVALUES

A. Volume scaling?

Since I have argued that the gauge coupling appears to be irrelevant, results from any gauge coupling anywhere in the deconfined phase (in the basin of attraction of the FP?) should be equally meaningful. I chose a gauge coupling $\beta = 5.2$ and $\kappa = 0.1285$. These are the second-smallest masses in Fig. 4. At this gauge coupling simulations are easy to perform. At this hopping parameter the IR cutoff (lattice volume) dominates the effect of the quark mass (the AWI mass is about 0.042). I computed the values of the lowest 8 eigenvalues of the Hermitian squared Dirac operator $D^\dagger D$, which I then converted into eigenvalues of the overlap operator by the usual stereographic projection. All of the configurations collected at this parameter value have zero topological charge. Results were shown in Fig. 1.

Two pictures illustrate the quality of the data, combined into Fig 6. The left panel shows simulation time histories of the lowest four eigenvalues of the 16^4 data set. Each measurement is separated by five HMC trajectories. The right panel shows the error on the average computed by blocking N_b successive measurements together. The lowest eigenvalue is clearly the noisiest, but the autocorrelation time seems not to be too large: I bin two successive lattices ($N_b = 2$ or $\Delta t = 10$ HMC units) together before averaging.

The spectrum is nothing like the spectrum of eigenvalues from a theory with chiral symmetry breaking, which consists of roughly equally spaced energy levels extending from the origin. The large spectral gap separating the lowest eigenvalue from the origin reflects the absence of chiral symmetry breaking in the weak coupling phase.

I repeated the calculation of eigenvalues using fundamental-representation valence quarks from a fundamental-representation simulation in the deconfined phase. The gauge coupling is $\beta = 5.5$ and $\kappa = 0.126$. This is a parameter set in which the screening masses have saturated at their Matsubara values. The picture is completely different – see Fig. 7. Again, there is a spectral gap, but now it is dominantly affected by the short (antiperiodic) length of the lattice, Matsubara physics again. The eigenvalue distribution does not depend simply on $L = V^{1/4}$.
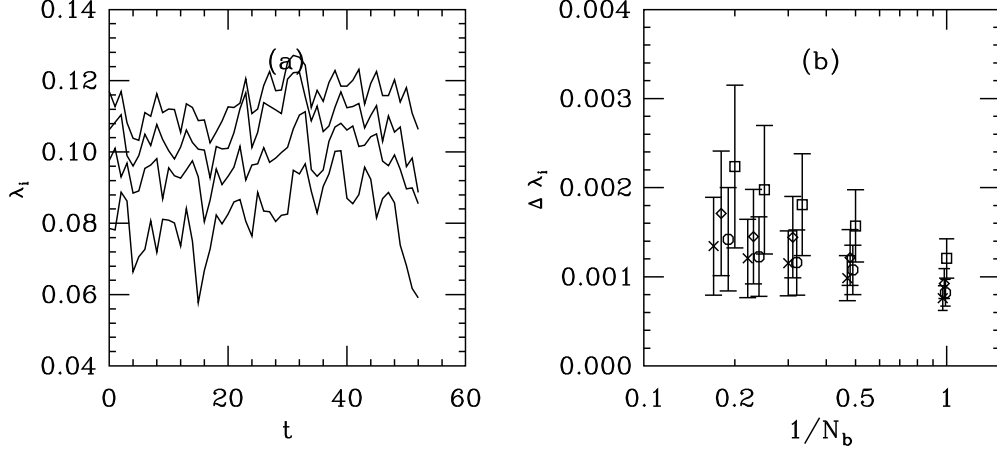
11

FIG. 6: (a) Time history of overlap eigenvalues from the 16^4 data set (in units of 5 HMC time steps). (b) Uncertainty on the average $\langle\lambda_i\rangle$ as a function of bin size. Symbols are squares for $i = 1$, octagons for $i = 2$, diamonds for $i = 3$, and crosses for $i = 4$.
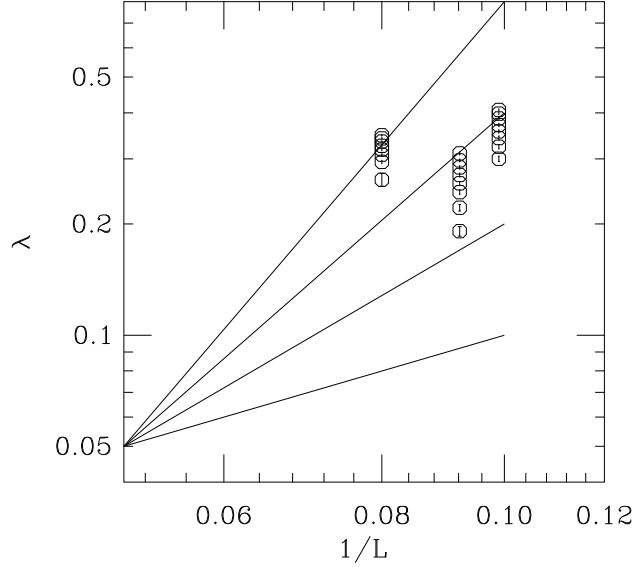

FIG. 7: Average value of ith eigenvalue of the fundamental-representation valence overlap operator, vs $1/L$, where the lattice volume V is defined to be $V = L^4$, from fundamental representation simulations. The actual volumes, moving from left to right across the graph, are $16^3 \times 6$, $12^3 \times 8$ and $12^3 \times 6$. The four lines are scaling curves $\langle\lambda_i\rangle L^p = $ constant, for $p = 4$, 3, 2, 1, from the top of the figure down.

Now let us try to extract an exponent from Fig. 1. This is not so easy: for theoretical input, all we have is Eq. 6, the finite-size scaling formula. One does not know a priori if it applies to all the eigenvalues or to only the lowest eigenvalues. One also does not know if there is some minimum volume for which it applies. (All of these questions have RMT answers for chirally-broken systems, but that is not what we are looking at here). So I will just proceed empirically: I will look at fits to individual eigenvalues, then groups of them. I

TABLE I: Exponent p from fits to individual eigenvalues, from the largest three volumes (16^4, $16^3 \times 8$, 12^4), or the largest four (add $12^3 \times 8$), or to all volumes (add $12^3 \times 6$).

	3 volumes		4 volumes		5 volumes	
mode	p	χ^2	p	χ^2	p	χ^2
1	1.11(12)	1.2	1.54(7)	19.8	1.42(5)	25.6
2	1.16(7)	10.1	1.39(5)	32.4	1.31(4)	37
3	1.36(5)	0.4	1.44(4)	5.8	1.47(3)	6.9
4	1.35(4)	4.0	1.41(3)	9.3	1.44(2)	11.3
5	1.46(4)	22	1.44(3)	22.7	1.49(2)	29
6	1.49(3)	57	1.44(2)	60.5	1.48(2)	67
7	1.52(3)	88	1.45(2)	101	1.48(2)	109
8	1.52(3)	100	1.44(2)	114	1.49(2)	129

will fit all the data sets or drop smaller volumes and fit only the larger ones.

I begin by fitting individual eigenvalues (lowest, second, and so on) to a power law, $\ln\langle\lambda_i\rangle = A_i - p\ln L$. I choose to fit to all five volumes, or four, or the largest three. The individual data points in each fit are uncorrelated, of course. Fits and chi-squareds are shown in Table I. Examples of fits are shown in Figs. 8 and 9.

Clearly, I can also fit groups of eigenvalues. In that case, I fit $\ln\langle\lambda_i\rangle = A_i - p\ln L$ for $i = 1 \ldots N$ eigenvalues. Now the data are correlated. I look at the quality of fits from uncorrelated fits, and then repeat by taking bootstrap averages of the data. The behavior is quite similar to the fits to individual eigenvalues. Some examples (with bootstrap errors) on the average, chi-squared from uncorrelated fits:

- Fit the lowest 4 eigenvalues and biggest 3 volumes: $p = 1.30(4)$, $\chi^2/dof = 25/(12-5)$

- Fit the lowest 4 eigenvalues biggest 4 volumes: $p = 1.42(3)$, $\chi^2/dof = 67/(16-5)$

- Fit all 8 eigenvalues and biggest 3 volumes: $p = 1.46(3)$, $\chi^2/dof = 331/(24-9)$

- Fit all 8 eigenvalues and biggest 4 volumes: $p = 1.43(2)$, $\chi^2/dof = 372/(32-9)$

Examples of these fits are shown in Fig. 10.

Generally, the fits are poor but the trend of the four-volume fits is clear: $p \sim 1.4$. I cannot assign an error which is not a guess: there are too many unknowns. Are the volumes large enough? Are the data sets large enough? Nobody has tried such an analysis before. I think it is better to present my results and let others explore new directions. Nevertheless, if the reader desires a number with an error bar, $p = 1.4(1)$ will capture the uncertainty over which fit to choose.

B. Additional properties of eigenvalues

Of course, there is more to the eigenvalue distribution than its average. In the absence of any theory, I will just compare cumulants, $C(x) = n(x)/N$ where $n(x)$ is the number of data points with a value smaller than x and N the total number of data points. I will rescale the
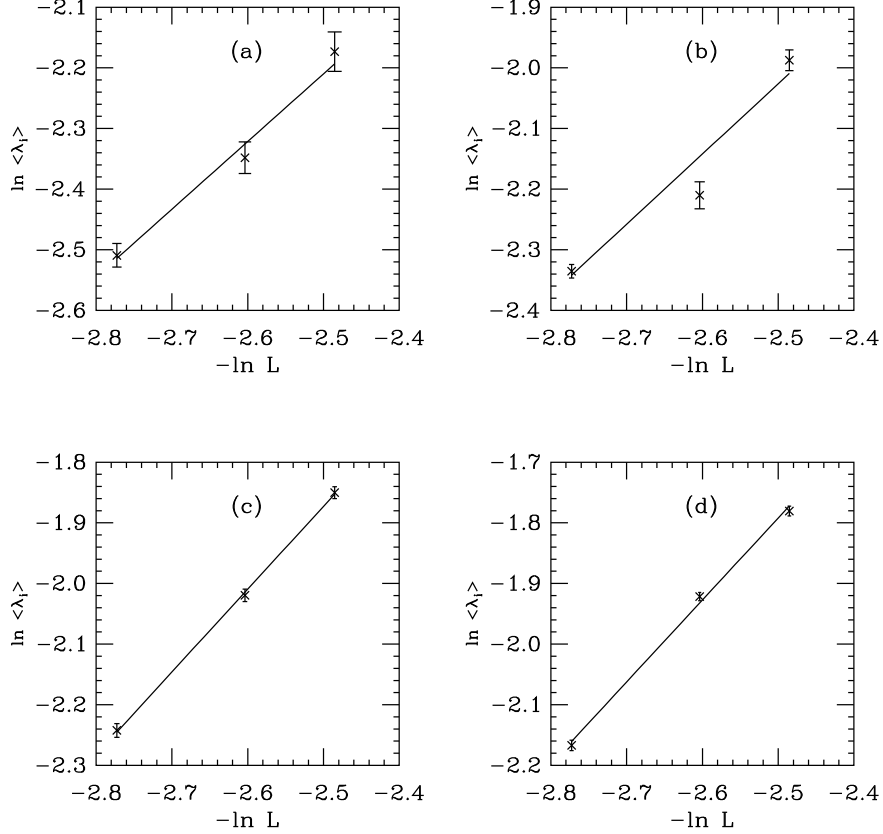
FIG. 8: Three-volume fits to individual eigenvalues, (a) the lowest eigenvalue (b) the first excited state (c) the second excited state (d) the third excited state. The volumes are (from the left) 16^4, $16^3 \times 8$ and 12^4.

data at each volume by a factor $(L_i/L_1)^p$ with $p = 1.4$ and $L_1 = 16$ in the plots. This is shown in Fig 11.

Apart from the lowest eigenvalue the cumulants are very sharp, indicating a strongly localized eigenvalue spectrum. This was observed by the authors of Ref. [9]. The lowest eigenvalue has a broad distribution. This is not surprising; the spectral gap is large and the "pressure" on it from all the higher eigenvalues is asymmetric. Could the broad distribution be related to the relatively poor scaling fits for this mode?

A direct calculation of $\rho(\lambda)$ involves histogramming the data. A possibly better technique is inspired by Ref. [56], namely to integrate the density

$$S(\Lambda) = \int_0^\Lambda \rho(\lambda)d\lambda \sim \Lambda^{\gamma+1}. \tag{12}$$

(basically the cumulant of all eigenvalues less than Λ). This was not a successful way to measure γ, since I did not have enough eigenmodes. Fig. 12 illustrates a typical data set, this time the $16^3 \times 8$ one. A few minutes with a ruler will produce a power law in the vicinity of 3 for $1 < S(\Lambda) < 8$ (compared to $4/y_m = 2.9$ for $y_m = 1.4$) but this is clearly only of entertainment value: the curve flattens when the data sets are exhausted, and presumably at lower Λ values the higher (missing) modes would contribute as well. Ref. [56] analyzed
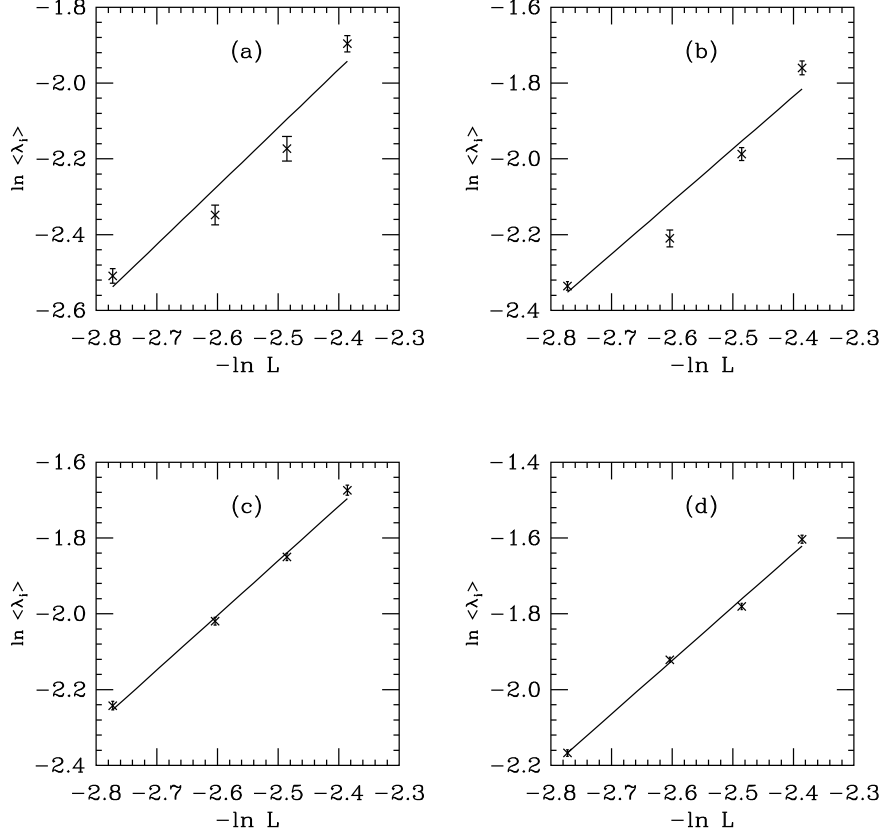
14

FIG. 9: Four-volume fits to individual eigenvalues, (a) the lowest eigenvalue (b) the first excited state (c) the second excited state (d) the third excited state. The volumes are (from the left) 16^4, $16^3 \times 8$, 12^4, and $12^3 \times 8$.

far more eigenvalues. I can collect several tens of eigenvalues of the squared clover Dirac operator quite easily, but the analysis did not seem to be crisp due to the explicit chiral symmetry breaking in the action, shifting the zero, and I did not pursue this as far as I probably should have.

At low Λ the plot shows a clear break. This is the part of the data which is completely dominated by the lowest eigenvalue, whose low-λ edge is not given by a simple power law. There must be interesting physics here (as there is for eigenvalue distributions of chirally broken systems) but I do not know what it is. I also do not know if this is real physics or just statistics: if $\rho(\lambda)$ is small in some region of λ, a big data set is needed to populate it.

V. DISCUSSION

Cautious readers might conclude that this paper is content-free: a curious Fig. 1 which appears only at the end of a long set of improbable constructions. In fact, I present the paper because Fig. 1 is so striking. Most of my analysis assumed that the underlying theory was conformal in the massless, infinite volume limit. I believe this assumption but it needs verification. Whether it is or not, one fact seems true: The deconfined phase of $SU(3)$ gauge theory with $N_f = 2$ flavors of sextet fermions seems to have quite different properties from
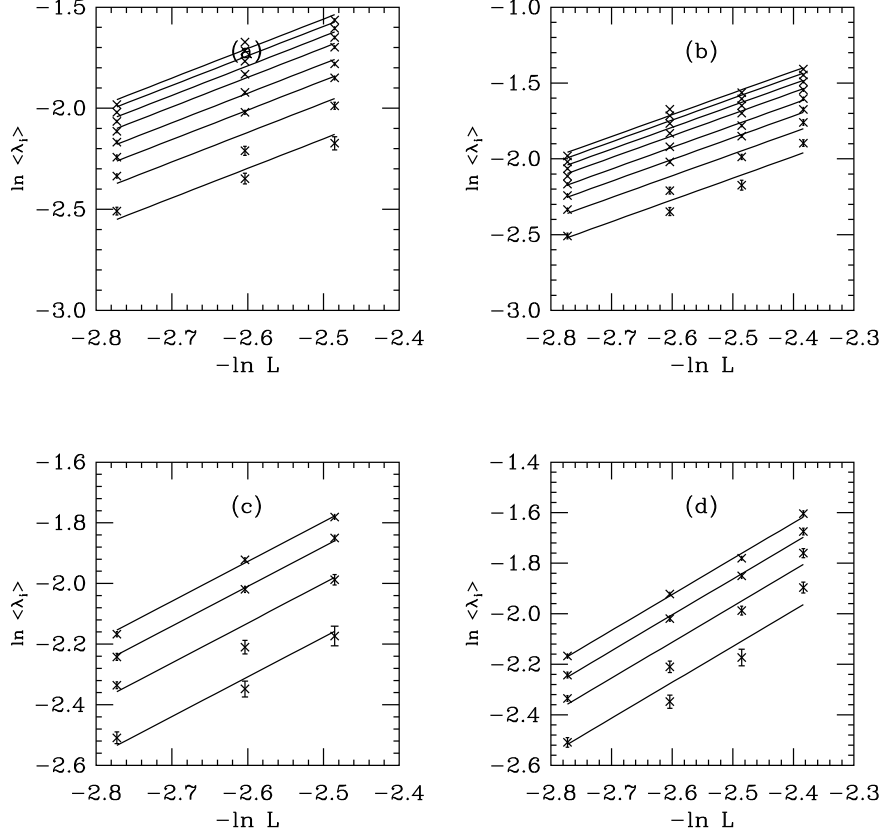
15

FIG. 10: Combined fits to several eigenvalues. (a) Three-volume fits to the 8 lowest eigenvalues, (b) four volume fits to the lowest 8 eigenvalues, (c) Three-volume fits to the lowest 4 eigenvalues, (d) four volume fits to the lowest 4 eigenvalues. The volumes are (from the left) 16^4, $16^3 \times 8$, 12^4 and in (b) and (d) $12^3 \times 8$.

the deconfined phase of $SU(3)$ gauge theory with $N_f = 2$ flavors of fundamental fermions.

Let us assume that the exponent I was measuring is truly what I claim it is: the leading exponent of a theory with one relevant coupling (the mass) which is critical at zero mass. As far as a lattice simulator can tell from reading the continuum literature, the answer $y_m \sim 1.4$ is very interesting: scaling exponents far from their engineering dimensions seem to be much sought after. (A partial subset of the literature is Refs. [57, 58, 59, 60, 61, 62].) Recalling that the exponent of the condensate is $\gamma = 4/y_m - 1$, this is an exponent of about $\gamma = 1.9(2)$.

A common prediction in the literature is that a lower bound on γ is $\gamma = 2$ or $y_m = 4/3$. The earliest appearance of this result I can find is by Cohen and Georgi [57], who obtain it by solving a gap equation. In a recent paper Kaplan, Lee and Son [62] argue on different grounds that γ should always exceed 2. My result is barely consistent with this prediction, with an uncertainty which in the end seems a bit inadequate.

Ryttov and Sannino [63] have a supersymmetric QCD - inspired beta function for gauge theories with higher dimensional representations of fermions. The anomalous dimension is predicted to be

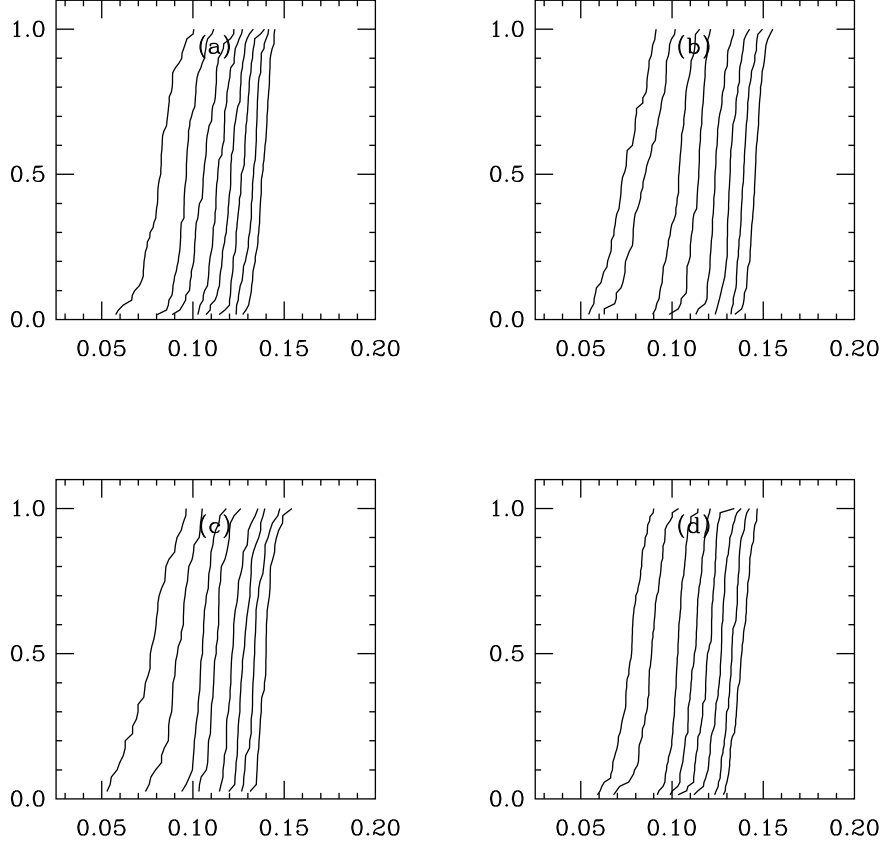$$\gamma = 3 - \frac{11C_2(G) - 4T(R)N_f}{2T(R)N_f} = 3 - \frac{13}{10} = 1.7. \tag{13}$$

16

FIG. 11: Cumulants, where the eigenvalue is rescaled by $(L_i/L_1)^p$ with $p = 1.4$ for the four largest volumes: (a) 16^4 (no rescaling) (b) $16^3 \times 8$ (c) 12^4 (d) $12^3 \times 8$.
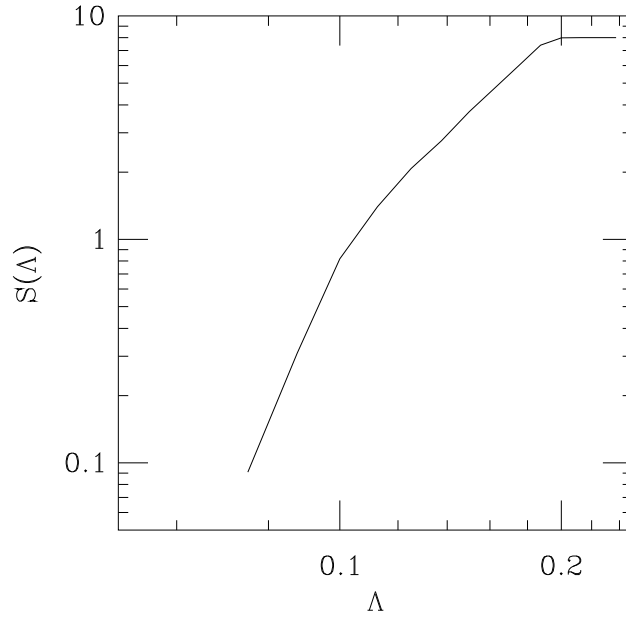

FIG. 12: $S(\Lambda)$ vs Λ (defined in Eq. 12) from the $16^3 \times 8$ data set.

There are some models of technicolor where the new physics sector is conformal or nearly so (for example [64, 65]); large anomalous dimensions (γ near 1) are desirable to achieve their phenomenological goals. This does not seem to be the case for sextet QCD.

The theoretical literature almost always addresses many models simultaneously, and validating (or otherwise) their assumptions requires data from many systems. y_m's for other lattice IRFP theories are needed.

From a simulation point of view, the present study could be improved by eliminating partial quenching. Perhaps the best candidate to do this is $SU(2)$ color with adjoint fermions. Codes may be fast enough to allow for simulations with dynamical overlap fermions on reasonable volumes.

A limitation of the use of eigenvalues is that at present, the theory is just finite size scaling. RMT predictions were rich because the number of theoretically motivated observables was large. Analysis like what I am doing needs additional theoretical input.

The published simulations of $N_f = 12$ fundamental fermions use staggered fermions. The technology for measuring susceptibilities for the condensate in the context of QCD thermodynamics is quite well developed. It would be interesting to apply it to present needs. Staggered fermion eigenvalues are also cheap to compute but explicit flavor breaking effects could hamper their interpretation.

Ultimately, the only universal quantities associated with IRFP theories are their critical exponents. Can lattice simulations measure them?

---

[1] P. H. Damgaard, U. M. Heller, A. Krasnitz and P. Olesen, Phys. Lett. B **400**, 169 (1997) [arXiv:hep-lat/9701008].

[2] U. M. Heller, Nucl. Phys. Proc. Suppl. **63**, 248 (1998) [arXiv:hep-lat/9709159].

[3] S. Catterall and F. Sannino, Phys. Rev. D **76**, 034504 (2007) [arXiv:0705.1664 [hep-lat]].

[4] T. Appelquist, G. T. Fleming and E. T. Neil, Phys. Rev. Lett. **100**, 171607 (2008) [arXiv:0712.0609 [hep-ph]].

[5] Y. Shamir, B. Svetitsky and T. DeGrand, Phys. Rev. D **78**, 031502 (2008) [arXiv:0803.1707 [hep-lat]].

[6] A. Deuzeman, M. P. Lombardo and E. Pallante, arXiv:0804.2905 [hep-lat].

[7] L. Del Debbio, A. Patella and C. Pica, arXiv:0805.2058 [hep-lat].

[8] S. Catterall, J. Giedt, F. Sannino and J. Schneible, JHEP **0811**, 009 (2008) [arXiv:0807.0792 [hep-lat]].

[9] Z. Fodor, K. Holland, J. Kuti, D. Nogradi and C. Schroeder, arXiv:0809.4888 [hep-lat].

[10] L. Del Debbio, A. Patella and C. Pica, arXiv:0812.0570 [hep-lat].

[11] T. DeGrand, Y. Shamir and B. Svetitsky, Phys. Rev. D **79**, 034501 (2009) [arXiv:0812.1427 [hep-lat]].

[12] A. J. Hietanen, J. Rantaharju, K. Rummukainen and K. Tuominen, JHEP **0905**, 025 (2009) [arXiv:0812.1467 [hep-lat]].

[13] G. T. Fleming, PoS **LATTICE2008**, 021 (2008) [arXiv:0812.2035 [hep-lat]].

[14] T. Appelquist, G. T. Fleming and E. T. Neil, arXiv:0901.3766 [hep-ph].

[15] A. J. Hietanen, K. Rummukainen and K. Tuominen, arXiv:0904.0864 [hep-lat].

[16] A. Deuzeman, M. P. Lombardo and E. Pallante, arXiv:0904.4662 [hep-ph].

[17] For a review of the phenomenology, see C. T. Hill and E. H. Simmons, Phys. Rept. **381**, 235 (2003) [Erratum-ibid. **390**, 553 (2004)] [arXiv:hep-ph/0203079].

[18] W. E. Caswell, Phys. Rev. Lett. **33**, 244 (1974).

[19] T. Banks and A. Zaks, Nucl. Phys. B **196**, 189 (1982).

[20] F. Sannino and K. Tuominen, Phys. Rev. D **71**, 051901 (2005) [arXiv:hep-ph/0405209].

[21] D. D. Dietrich and F. Sannino, Phys. Rev. D **75**, 085018 (2007) [arXiv:hep-ph/0611341].

[22] T. A. Ryttov and F. Sannino, Phys. Rev. D **76**, 105004 (2007) [arXiv:0707.3166 [hep-th]].

[23] For a review, see T. DeGrand and A. Hasenfratz, arXiv:0906.1976 [hep-lat].

[24] G. Mack, Commun. Math. Phys. **53**, 155 (1977).

[25] H. Leutwyler and A. V. Smilga, Phys. Rev. D **46**, 5607 (1992).

[26] F. Karsch [RBC-Bielefeld collaboration], Nucl. Phys. A **820**, 99C (2009) [arXiv:0810.3078 [hep-lat]].

[27] See the discussion in C. DeTar and U. M. Heller, arXiv:0905.2949 [hep-lat].

[28] T. Banks and A. Casher, Nucl. Phys. B **169**, 103 (1980).

[29] G. Akemann, P. H. Damgaard, U. Magnea and S. M. Nishigaki, Nucl. Phys. B **519**, 682 (1998) [arXiv:hep-th/9712006].

[30] B. Sheikholeslami and R. Wohlert, Nucl. Phys. B **259**, 572 (1985).

[31] A. Hasenfratz, R. Hoffmann and S. Schaefer, JHEP **0705**, 029 (2007) [arXiv:hep-lat/0702028].

[32] M. Hasenbusch, Phys. Lett. B **519**, 177 (2001) [arXiv:hep-lat/0107019].

[33] C. Urbach, K. Jansen, A. Shindler and U. Wenger, Comput. Phys. Commun. **174**, 87 (2006) [arXiv:hep-lat/0506011].

[34] T. Takaishi and P. de Forcrand, Phys. Rev. E **73**, 036706 (2006) [arXiv:hep-lat/0505020].

[35] A. Hasenfratz, R. Hoffmann and S. Schaefer, Phys. Rev. D **78**, 054511 (2008) [arXiv:0806.4586 [hep-lat]].

[36] http://www.physics.utah.edu/%7Edetar/milc/

[37] T. Blum *et al.* [RBC Collaboration], Phys. Rev. D **68**, 114506 (2003) [arXiv:hep-lat/0110075].

[38] Y. Aoki *et al.*, Phys. Rev. D **73**, 094507 (2006) [arXiv:hep-lat/0508011].

[39] C. Allton *et al.* [RBC and UKQCD Collaborations], Phys. Rev. D **76**, 014504 (2007) [arXiv:hep-lat/0701013].

[40] C. A. Aubin, J. Laiho, and R. S. Van de Water, arXiv:0710.1121 [hep-lat].

[41] H. Neuberger, Phys. Lett. B **417**, 141 (1998) [arXiv:hep-lat/9707022].

[42] H. Neuberger, Phys. Rev. Lett. **81**, 4060 (1998) [arXiv:hep-lat/9806025].

[43] T. A. DeGrand [MILC collaboration], Phys. Rev. D **63**, 034503 (2001) [arXiv:hep-lat/0007046].

[44] T. A. DeGrand and S. Schaefer, Phys. Rev. D **71**, 034507 (2005) [arXiv:hep-lat/0412005].

[45] T. DeGrand and S. Schaefer, JHEP **0607**, 020 (2006) [arXiv:hep-lat/0604015].

[46] T. DeGrand and S. Schaefer, Phys. Rev. D **76**, 094509 (2007) [arXiv:0708.1731 [hep-lat]].

[47] T. DeGrand, Z. Liu and S. Schaefer, Phys. Rev. D **74**, 094504 (2006) [Erratum-ibid. D **74**, 099904 (2006)] [arXiv:hep-lat/0608019].

[48] A. Stathopoulos, SIAM J. Sci. Comput., Vol. 29, No. 2, (2007), 481–514; A. Stathopoulos and

J. R. McCombs, SIAM J. Sci. Comput., Vol. 29, No. 5, (2007), 2162-2188.

[49] U. M. Heller, R. G. Edwards and R. Narayanan, Nucl. Phys. Proc. Suppl. **73**, 497 (1999) [arXiv:hep-lat/9810003].

[50] M. Garcia Perez, A. Gonzalez-Arroyo and A. Sastre, PoS **LAT2007**, 328 (2007) [arXiv:0710.0455 [hep-lat]].

[51] D. Nógrádi, talk at the Institute for Nuclear Theory workshop "New Frontiers in Large N Gauge Theories," Seattle, February 2009.

[52] J. C. Myers and M. C. Ogilvie, arXiv:0903.4638 [hep-th].

[53] O. Machtey, Y. Shamir, and B. Svetitsky, private communication.

[54] Recent compilations of screening masses in high temperature QCD include E. Laermann, A. Francis, S. Fröhlich, and S. Mukherjee, PoS (Lattice 2008) 193; S. Wissel, E. Laermann, S. Shcheredin, S. Datta and F. Karsch, PoS **LAT2005**, 164 (2006) [arXiv:hep-lat/0510031].

[55] C. DeTar, PoS **LAT2008**, 001 (2008) [arXiv:0811.2429 [hep-lat]].

[56] L. Giusti and M. Luscher, JHEP **0903**, 013 (2009) [arXiv:0812.3638 [hep-lat]].

[57] A. G. Cohen and H. Georgi, Nucl. Phys. B **314**, 7 (1989).

[58] J. Braun and H. Gies, JHEP **0606**, 024 (2006) [arXiv:hep-ph/0602226].

[59] T. Appelquist, J. Terning and L. C. R. Wijewardhana, Phys. Rev. Lett. **77**, 1214 (1996) [arXiv:hep-ph/9602385].

[60] T. Appelquist, A. Ratnaweera, J. Terning and L. C. R. Wijewardhana, Phys. Rev. D **58**, 105017 (1998) [arXiv:hep-ph/9806472].

[61] E. Gardi and G. Grunberg, JHEP **9903**, 024 (1999) [arXiv:hep-th/9810192].

[62] D. B. Kaplan, J. W. Lee, D. T. Son and M. A. Stephanov, arXiv:0905.4752 [hep-th].

[63] T. A. Ryttov and F. Sannino, Phys. Rev. D **78**, 065001 (2008) [arXiv:0711.3745 [hep-th]].

[64] M. A. Luty and T. Okui, JHEP **0609**, 070 (2006) [arXiv:hep-ph/0409274].

[65] M. A. Luty, JHEP **0904**, 050 (2009) [arXiv:0806.1235 [hep-ph]].